



## Research Paper

# Gap Junctions Contribute to Ictal/Interictal Genesis in Human Hypothalamic Hamartomas



Jie Wu<sup>a,b,c,\*,1</sup>, Ming Gao<sup>b</sup>, Stephen G. Rice<sup>d</sup>, Candy Tsang<sup>d</sup>, John Beggs<sup>b</sup>, Dharshaun Turner<sup>b</sup>, Guohui Li<sup>b</sup>, Bo Yang<sup>a</sup>, Kunkun Xia<sup>a,b</sup>, Fenfei Gao<sup>c</sup>, Shenfeng Qiu<sup>e</sup>, Qiang Liu<sup>b</sup>, John F. Kerrigan<sup>d,1</sup>

<sup>a</sup> The First Affiliated Hospital of Zhengzhou University, Zhengzhou, Henan 450052, China

<sup>b</sup> Division of Neurology, Barrow Neurological Institute, St. Joseph's Hospital and Medical Center, Phoenix, AZ 85013, USA

<sup>c</sup> Department of Pharmacology, Shantou University of Medical College, Guangdong, Shantou 815041, China

<sup>d</sup> Division of Pediatric Neurology, Barrow Neurological Institute, Phoenix Children's Hospital, Phoenix, AZ 85016, USA

<sup>e</sup> Department of Basic Medical Sciences, University of Arizona College of Medicine, Phoenix, AZ 85004, USA

## ARTICLE INFO

## Article history:

Received 20 February 2016

Received in revised form 21 April 2016

Accepted 21 April 2016

Available online 22 April 2016

## Keywords:

Human epilepsy

Hypothalamic hamartoma

Gelastic seizures

Patch-clamp

Gap junction

## ABSTRACT

Human hypothalamic hamartoma (HH) is a rare subcortical lesion associated with treatment-resistant epilepsy. Cellular mechanisms responsible for epileptogenesis are unknown. We hypothesized that neuronal gap junctions contribute to epileptogenesis through synchronous activity within the neuron networks in HH tissue. We studied surgically resected HH tissue with Western-blot analysis, immunohistochemistry, electron microscopy, biocytin microinjection of recorded HH neurons, and microelectrode patch clamp recordings with and without pharmacological blockade of gap junctions. Normal human hypothalamus tissue was used as a control. Western blots showed increased expression of both connexin-36 (Cx36) and connexin-43 (Cx43) in HH tissue compared with normal human mammillary body tissue. Immunohistochemistry demonstrated that Cx36 and Cx43 are expressed in HH tissue, but Cx36 was mainly expressed within neuron clusters while Cx43 was mainly expressed outside of neuron clusters. Gap-junction profiles were observed between small HH neurons with electron microscopy. Biocytin injection into single recorded small HH neurons showed labeling of adjacent neurons, which was not observed in the presence of a neuronal gap-junction blocker, mefloquine. Microelectrode field recordings from freshly resected HH slices demonstrated spontaneous ictal/interictal-like discharges in most slices. Bath-application of gap-junction blockers significantly reduced ictal/interictal-like discharges in a concentration-dependent manner, while not affecting the action-potential firing of small gamma-aminobutyric acid (GABA) neurons observed with whole-cell patch-clamp recordings from the same patient's HH tissue. These results suggest that neuronal gap junctions between small GABAergic HH neurons participate in the genesis of epileptic-like discharges. Blockade of gap junctions may be a new therapeutic strategy for controlling seizure activity in HH patients.

© 2016 The Authors. Published by Elsevier B.V. This is an open access article under the CC BY-NC-ND license (<http://creativecommons.org/licenses/by-nc-nd/4.0/>).

## 1. INTRODUCTION

Human hypothalamic hamartomas (HHs) are developmental malformations occurring in the ventral hypothalamus. HHs are associated with neurological and endocrine disorders, including intractable seizures, cognitive impairment, behavioral disturbances, and central precocious puberty (Berkovic et al., 1988; Kerrigan et al., 2005). The epileptic syndrome in HH patients is characterized by laughing (gelastic) seizures, often beginning in early infancy. Most patients with gelastic

seizures have a progressive natural history, and later develop additional seizure types and cognitive and psychiatric comorbidities (Berkovic et al., 1988; Prigatano et al., 2008). Seizures associated with HH are usually refractory to standard anti-epilepsy drugs, but surgical treatment can be effective (Mittal et al., 2013). Multiple clinical studies have demonstrated that HHs are intrinsically epileptogenic (Kuzniecky et al., 1997; Munari et al., 1995). However, cellular and molecular mechanisms underlying epileptogenesis within HH lesions remain incompletely understood (Wu et al., 2015).

Gap junctions are cell-to-cell channel-forming structures formed by specialized proteins (connexins) in the plasma membranes of adjacent cells. They allow direct electrical coupling and chemical communication between almost all cell types in the central nervous system. Many different connexin proteins have been identified; most are specific for different cell types in the brain, including neurons and glia (Nakase et al.,

\* Corresponding author at: Division of Neurology, Director of Neurophysiology Laboratory, Barrow Neurological Institute, St. Joseph's Hospital and Medical Center, 350 W. Thomas Road, Phoenix, AZ 85013-4496, U.S.A.

E-mail address: [jie.wu@dignityhealth.org](mailto:jie.wu@dignityhealth.org) (J. Wu).

<sup>1</sup> Drs. Wu and Kerrigan contributed equally as corresponding authors for this paper.

2004; Rozental et al., 2000). Connexin-36 (Cx36) is predominantly expressed in gamma-aminobutyric acid-ergic (GABAergic) interneurons (Cruikshank et al., 2005; Sohl et al., 2005). In the rat, Cx36 shows a high level of expression in the hypothalamus, including the mammillary bodies (Condorelli et al., 2000). Gap junctions play an important role in locally synchronizing GABAergic neuron activity, including action-potential firing and sub-threshold changes in transmembrane potential resulting from inhibitory and excitatory post-synaptic potentials (Cruikshank et al., 2005). Gap junctions contribute to oscillating field potentials and enable GABAergic entrainment of principal (projection) neuron behavior within normal networks (Sohl et al., 2005).

In view of these functional features, gap junctions likely contribute to the pathogenesis of epilepsy, particularly with respect to enhancing synchronous activity of neuronal subgroups within epileptic networks (Carlen et al., 2000; Dudek et al., 1998; Traub et al., 2004). This concept is supported by in vitro and in vivo epileptic animal models, in which the pharmacological blockade of gap junctions significantly reduces seizure occurrence (Carlen et al., 2000; Traub et al., 2004). Interictal epileptiform discharges (in the form of fast oscillations) can be abolished in freshly resected human epileptic tissue slices with carbenoxolone, a non-specific gap-junction blocker (Roopun et al., 2010). However, the understanding of gap junctions in human epileptogenesis is still limited and the potential for gap-junction blockers as therapeutic agents for human epilepsy remains effectively unexplored.

We hypothesized that neuronal gap junctions have a mechanistic role in synchronizing neuronal firing and contributing to seizure onset in human HH. We evaluated the role of gap junctions in epileptogenesis using multiple experimental approaches including Western-blot, immunohistochemical staining, electron microscopy and electrophysiology in HH tissue surgically resected from patients with treatment-resistant gelastic seizures. We found that HH tissue expressed significantly higher level of Cx36 and Cx43 compared to normal control hypothalamic tissue, and pharmacological block of gap junctions significantly reduced seizure-like discharges in HH slices.

## 2. Materials and Methods

### 2.1. Informed Consent

Written informed consent for use of post-surgical tissue for research purposes was obtained under protocols approved by the institutional review boards at Barrow Neurological Institute, St. Joseph's Hospital and Medical Center, and Barrow Neurological Institute at Phoenix Children's Hospital (Phoenix, Arizona).

### 2.2. Patient Profile

Surgically resected HH tissue was obtained from 27 patients (15 males, 56%) treated between July 2003 and April 2013 (mean age at surgery, 10.3 years; range, 0.7–36.8 years). All patients had treatment-resistant epilepsy and a history of gelastic seizures. At the time of surgery, nine (33%) had only gelastic seizures, while 18 (67%) had multiple seizure types, including complex partial seizures (Kim et al., 2009), generalized tonic-clonic (nine), myoclonic (two), atonic (two), and infantile spasms (one). Twenty-five patients (93%) had at least one seizure per day, while two (7%) had at least one seizure per month. Intellectual disability or developmental retardation (intelligence quotient or developmental quotient < 70) was present in 13 patients (48%) and prior history of central precocious puberty was present in nine (33%). None of the patients in this cohort had identified genetic syndromes. Classification of HH lesions according to the method of Delalande and Fohlen (Delalande et al., 2003) showed eight Type I (30%), nine Type II (33%), seven Type III (26%), and three Type IV (11%) lesions. Mean lesion volume was 2.7 cm<sup>3</sup> (range, 0.2–14.8 cm<sup>3</sup>).

### 2.3. Control Tissue

Normal human hypothalamic control tissues were obtained from the U.S. National Institute of Child Health and Human Development (NICHD) Brain and Tissue Bank for Developmental Disorders at the University of Maryland (Baltimore, MD).

### 2.4. Immunohistochemical Staining for Connexins in HH Tissue

HH tissue was sectioned into 4- $\mu$ m slices. Tissue was deparaffinized and antigen retrieval was performed using 10 mM of sodium citrate buffer, washed with phosphate-buffered saline (PBS), blocked for 1 h at room temperature in 4% normal serum, 4% bovine serum albumin (BSA), and 0.4% Triton X in PBS. The tissue was incubated overnight at 4 °C with the primary antibody. Separate sections were stained for Cx36 1:150 (Abcam, Cambridge, MA) and Cx43 1:3000 (Abcam), each double-labeled with NeuN 1:500 (Millipore, Billerica, MA). Slides were incubated with goat anti-rabbit conjugated Alexa 594 and goat anti-mouse conjugated Alexa 488 (Invitrogen, Carlsbad, CA) secondary antibodies for 2 h at room temperature.

### 2.5. Western-blot Analysis of Connexin Expression in HH Tissue

Tissue samples were sonicated in RIPA buffer (150 mM NaCl, 1% Triton X-100, 0.1% SDS, 0.5% Na deoxycholate, 50 mM Tris), and total protein was determined using BCA protein assays (Thermo-Scientific, Waltham, MA). Experiments were performed on the XCell II Blot Module (Invitrogen). From each sample, 20  $\mu$ g of protein was loaded into a lane on a NuPage 4–12% Bis-Tris gel (Life Technologies, Carlsbad, CA), transferred to 0.2- $\mu$ m polyvinylidene difluoride membrane (Bio-Rad, Hercules, CA), and processed with a blocking solution of 3% BSA and 5% nonfat dry milk in 1  $\times$  tris-buffered saline and Tween-20 (TBST). Rabbit anti-Cx36 (0.5  $\mu$ l/ml; Invitrogen), rabbit anti-Cx43 (0.2  $\mu$ l/ml; Invitrogen), and mouse anti-tubulin (1:10,000; Sigma-Aldrich, St. Louis, MO) were used as primary antibodies, and were visualized with horseradish peroxidase-conjugated anti-rabbit antibody (1:10,000; Invitrogen) or anti-mouse IgG antibody (1:10,000; Sigma-Aldrich). Signals were enhanced using enhanced chemiluminescence detection reagents (Thermo-Scientific) and detected on a BioSpectrum imaging system (UVP, Upland, CA). Densities were quantified using VisionWorks (UVP) and normalized relative to tubulin.

### 2.6. Electron Microscopy (EM) Analysis of Gap Junction Profiles in HH Tissue

**Tissue processing:** Up to three pieces of tissue (1–3 mm in diameter) were provided for ultrastructural examination, fixed overnight in 3% phosphate-buffered glutaraldehyde, post-fixed for 2 h with 2% phosphate-buffered osmium tetroxide, dehydrated with a series of graded ethanols and propylene oxide, and embedded in epoxy resin (LX-112, Ladd Research, Williston, VT). Thin tissue sections were cut with a diamond knife (Diatome AG, Biel, Switzerland), mounted on 150-mesh copper grids (Ted Pella, Redding, CA), and stained with lead citrate and uranyl acetate. Serial sections for three-dimensional reconstructions were mounted on polyvinyl formal-coated grids with a single slot (1  $\times$  2 mm).

**Image processing:** Sections were examined with a Philips CM100 equipped with a CompuStage (FEI Company, Hillsboro, OR). Images were captured with an Orius SC1000 camera (Gatan, Pleasanton, CA).

### 2.7. Fresh HH Slice Preparation

Surgically resected HH slices were prepared based on our published protocol (Wu et al., 2005). Briefly, fresh HH-tissue sections obtained at the time of surgery were immediately placed in ice-cold dissection solution (2–4 °C), which contained (in mM) 136.7 NaCl, 5 KCl, 0.1 NaH<sub>2</sub>PO<sub>4</sub>,

9.84 *N*-2-hydroxyethylpiperazine-*N'*-2-ethanesulfonic acid (HEPES), 16.6 glucose, and 21.9 sucrose; the sections were continuously bubbled with carbogen (95% O<sub>2</sub>/5% CO<sub>2</sub>; pH 7.4) during delivery from the operating room to the research laboratory. The tissue sections were quickly sliced into several smaller pieces (250- $\mu$ m thick for whole-cell patch-clamp recording and 450–500- $\mu$ m thick for field recording) using a Vibratome (Vibratome Company, St. Louis, MO) and were bubbled with carbogen at 35 °C for 30 min in an incubation solution (in mM: 124 NaCl, 5 KCl, 24 NaHCO<sub>3</sub>, 1.3 MgSO<sub>4</sub>, 1.2 KH<sub>2</sub>PO<sub>4</sub>, 2.4 CaCl<sub>2</sub>, 10 glucose), and then further incubated at room temperature (22  $\pm$  1 °C) for at least 1 h.

### 2.8. Electrophysiological Recordings in Fresh HH Slices

Standard extracellular field potential recordings were performed in thick (450  $\mu$ m) HH slices using borosilicate glass micropipettes filled with 2 M NaCl. The recording temperature was set to 34  $\pm$  1 °C. For each HH slice, we scanned at least 16 recording sites (4  $\times$  4) with 500- $\mu$ m distance. The spontaneous seizure-like discharges were recorded using an Axoclamp-2B amplifier (Axon Instruments, Inc., Union City, CA).

To measure HH neuron action potential, whole-cell patch-clamp recording in current-clamp mode from HH slices (250  $\mu$ m) was performed, and the pipette solution contained (in mM) 130 mM KMeSO<sub>4</sub>, 10 mM KCl, 10 mM HEPES/K-HEPES, 2 mM MgSO<sub>4</sub>, 0.5 mM EGTA, and 3 mM ATP; the pH was adjusted to 7.3 with KOH.

### 2.9. Statistics

All statistical experimental results are presented as mean  $\pm$  SEM except the use of medians and quartiles to quantify Western blot data. The Student's *t*-test (parametric data) or Mann Whitney *U* test (non-parametric data) was used to compare two groups; multiple comparisons were performed using one-way analysis of variance (ANOVA), Chi square test was used to compare cell numbers between two groups of patch-clamp recordings with and without gap junction blocker. Statistical significance was set at  $p < 0.05$ .

## 3. Results

### 3.1. Expression of Gap Junction Proteins in Human HH Tissue

To determine whether gap junction proteins are expressed in human HH tissue, we performed immunohistochemical staining to explore expression of Cx36 (neuronal) and Cx43 (glial) connexin proteins (eight patients for each). All HH tissues (100%) expressed Cx36 and

Cx43. Fig. 1 demonstrates the results from triple immunohistochemical staining, in which red indicated either Cx36 in left panel or Cx43 in right panel, green indicated NeuN staining for neurons, and blue indicated DAPI staining for all cell nucleus. Results showed that all HH sections tested showed differences in the regional distribution of connexin proteins—Cx36 showed more abundant staining intensity within neuron clusters, while Cx43 was more abundant within the neuron-poor region (as shown by co-labeling with NeuN, which stains all neurons, and DAPI, which stains all nucleated cells including glia) (Fig. 1).

### 3.2. Enhanced Expression of Gap Junction Proteins in Human HH Tissue

To determine if the expression of gap junction proteins is altered relative to adjacent control tissue, we performed Western-blot assays to quantitatively compare Cx36 and Cx43 protein levels between human HH tissue and age-matched human autopsy control tissue (mammillary body) (eight subjects versus eight control specimens for each study). Connexin levels were normalized to tubulin levels for all samples. Fig. 2A demonstrates a typical gel data from 3 control and 4 HH patients (HH number is patient ID for research). Statistical analysis showed significant increased expression ( $p < 0.05$  by Mann Whitney *U* test for non-parametric data) of both Cx36 and Cx43 in epileptic HH tissue ( $n = 8$  patients) versus normal controls ( $n = 8$  cases) (Fig. 2B). Panel I shows a striking co-localization of Cx36 within the cluster of small HH neurons as indicated by green staining with NeuN (panel IB) and very little Cx36 immunoreactivity in regions without neurons (panel IA). In Panel II, conversely, Cx43 co-localizes in regions of the tissue with many glia and few neurons (panel IIC) with less expression within neuron clusters (panel IID). Thus, the protein expression level of Cx36 (neuronal) gap junction is higher in epileptic HH tissue relative to adjacent normal hypothalamus.

### 3.3. Ultrastructural Evidence of Gap Junction Profiles between Small HH Neurons

We used electron microscopy to detect the presence of gap-junction profiles in HH sections, with particular attention to the phenotype of the cellular pair contributing to the gap junction (seven cases). While trilaminar gap-junction profiles were present, it was challenging to make this visual determination in such a way that the phenotype of both cells could be determined with complete certainty, as many such profiles were indeterminate. In four of the seven HH cases (57%) studied, we found at least one trilaminar gap-junction profile connecting adjacent small HH neurons (Fig. 3).

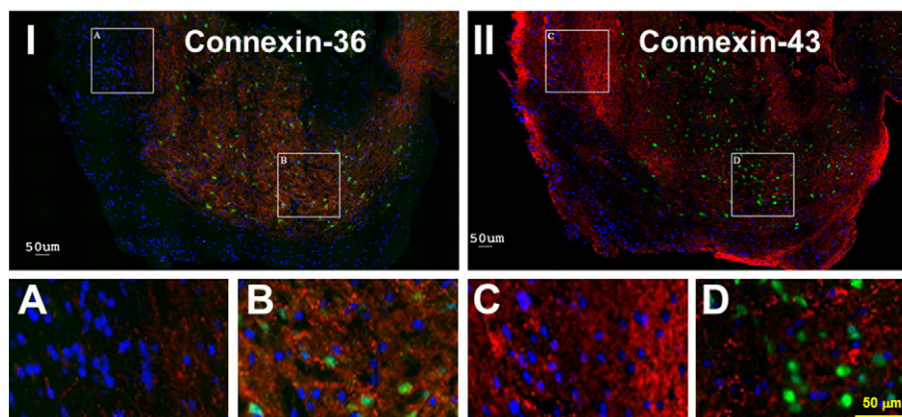


**Fig. 1.** A representative case showing immunohistochemistry for Cx36 (neuronal) and Cx43 (glial) proteins in surgically resected human HH tissue. Triple staining was applied: red for antibodies to either Cx36 (panel I) or Cx43 (panel II), green for the antibody to NeuN (both panels), and blue for reactivity with DAPI (both panels). The scale bar in IID also applies to IA, IB, and IIC.

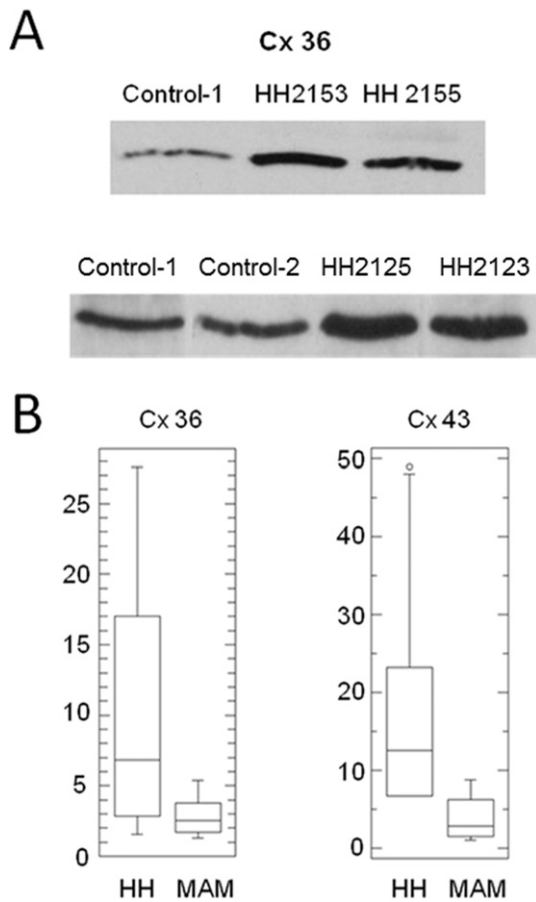


**Fig. 2.** Boxplot of Western-blot study of connexin protein levels within HH tissue (HH) versus human age-matched autopsy control mammillary body tissue (MAM). (A) A typical gel data from 3 control and 4 HH patients (HH number is patient ID for research) showed enhanced level of Cx36 in HH tissues compared to control tissues. (B) Expression levels are normalized to tubulin expression. Expression of Cx36 levels (left panel) in HH were significantly higher than in MAM control tissue ( $p = 0.04$ ; Mann-Whitney) and expression of Cx43 (right) in HH was significantly higher than in MAM control tissue ( $p = 0.005$ ; Mann-Whitney). Data are presented as follows: bar within box = median, upper edge of box = third quartile, lower edge of box = first quartile, upper whisker = maximum, lower whisker = minimum, open circle = outlier ( $>3\times$  expected range of variation).

### 3.4. Functional Evidence for the Presence of Gap Junctions

To establish the presence of functional gap junctions between small HH neurons, we performed whole-cell patch-clamp recordings in HH slices. Under DIC-interfering microscope, we identified small HH

neurons as round cells (soma diameter  $< 20 \mu\text{m}$ ) with spontaneous action potential firing, consistent with the expected phenotype (Wu et al., 2005). We injected biocytin into the recorded neurons, followed by a depolarizing protocol (repetitive application of depolarizing current of 30–50 pA into recorded neurons for 3–5 min), which promotes the opening of gap junctions. In 23 small HH neurons tested (from 12 patients), 17 recorded neurons showed multiple adjacent biocytin labeled neurons (neuron pairs) and 6 neurons showed single labeled neuron (Fig. 4A–B). The average of labeled cell number per biocytin injection was  $2.6 \pm 0.3$ . However, in the presence of the neuronal (Cx36) gap-junction blocker, mefloquine (10  $\mu\text{M}$ ), no labeling of adjacent neurons (neuron pairs) was observed in 11 injected small HH neurons (from six patients) (Fig. 4C–D). Statistical analysis of labeled neuronal numbers in the group without mefloquine vs. with mefloquine ( $2.6 \pm 0.3$  vs. 1) demonstrated significant difference (Chi-square Test: Chi-square = 16.3 with 4 degrees of freedom, and  $p = 0.003$ ). These results are consistent with the presence of functional gap junctions that couple small HH neurons.

### 3.5. Effects of Neuronal Gap-junction Blocker on Ictal/Interictal-like Discharges in HH Slices

Results presented thus far support the premise that functional gap junctions are highly expressed in human HH tissue. To explore the possible role of gap junctions in ictal/interictal genesis, we examined the effects of neuronal type gap-junction blocker, mefloquine on spontaneous ictal/interictal-like discharges in HH slices using field potential recordings because mefloquine is known as a relatively selective neuronal (Cx36) gap-junction blocker (Juszczak et al., 2009). Fig. 5 shows results from 8 HH tissue slices prepared from four patients with spontaneous ictal/interictal-like discharges (Fig. 5Aa). Bath-application of 10  $\mu\text{M}$  mefloquine for 20 min dramatically eliminated these spontaneous ictal/interictal-like discharges (Fig. 5Ab). After washout for 10–30 min, these spontaneous ictal/interictal-like discharges could be recovered (Fig. 5A,c). In parallel experiments on HH tissue slices prepared from the same patient (but not from the same HH slice), whole-cell patch-clamp recordings showed that the spontaneous action potential firing of small HH neurons was not affected by 10  $\mu\text{M}$  mefloquine (Fig. 5B), suggesting that mefloquine blocks ictal/interictal-like discharges by interrupted network synchronization, but not by blocking spontaneous action potential firing in individual small HH neurons. Statistical analysis from eight HH slices tested (from four patients) demonstrated a significant reduction of bursting numbers ( $p < 0.001$ , paired  $t$ -test) and amplitude ( $p < 0.001$ , paired  $t$ -test) by bath-perfusion of 10  $\mu\text{M}$  mefloquine (Fig. 5C). These results suggest that pharmacological block of neuronal gap junction eliminates ictal/interictal activity in human HH slices.

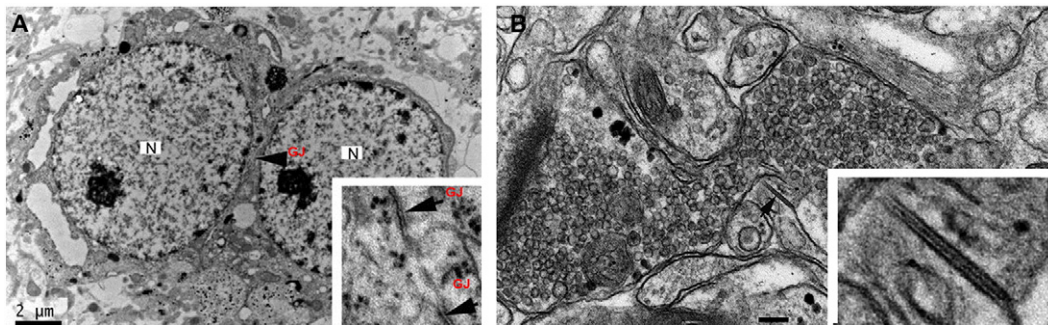


**Fig. 3.** (A) Electron photomicrograph of two adjacent small HH neurons. The nuclei (N) are relatively large with a single dense nucleolus, surrounded by a relatively thin rim of cytoplasm, defining the cell body. These are the expected features for small HH neurons (as described by Beggs et al., 2008; Parvizi et al., 2011). Specialized non-synaptic junctions (possible gap-junction profiles; GJ) can be observed between the soma of these two neurons (see inset). (B) A gap junction profile (arrow) with tri-laminar structure between neurites in close proximity to a large axon terminal filled with synaptic vesicles. The inset shows greater detail of the gap junction. Our staining method shows that dense material connects adjacent plasma membranes.

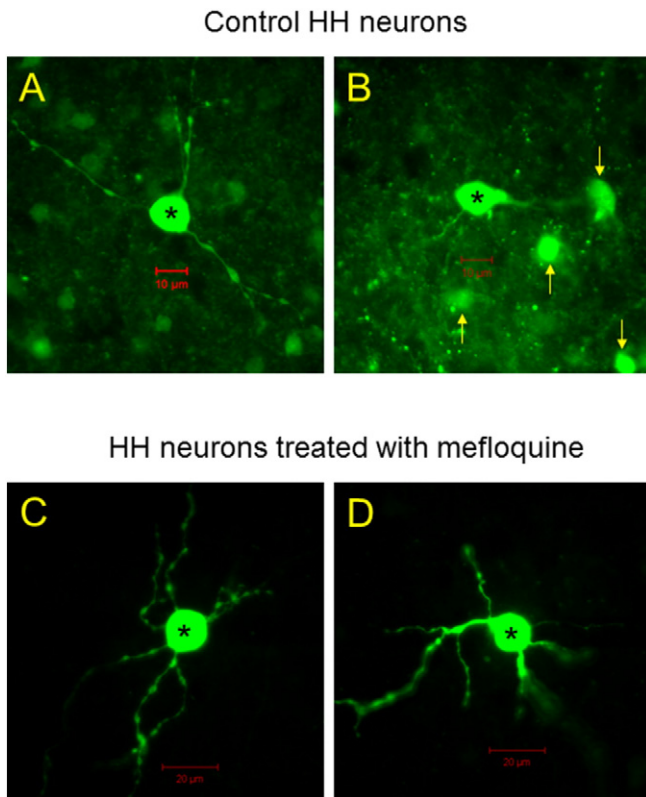


**Fig. 4.** (A–B) Photomicrograph of an injected small HH neuron subsequent to whole-cell patch-clamp microelectrode recording (WC patch). Filling the recorded cell with biocytin has also filled multiple adjacent cells, likely other small HH neurons. (C–D) Photomicrographs of two small HH neurons injected with biocytin after microelectrode recording in the presence of mefloquine, a gap-junction blocker that is relatively specific for neuronal gap junctions. In the presence of mefloquine, adjacent neurons were not labeled.

### 3.6. Effects of Carbenoxolone on Ictal/interictal-like Discharges in HH Slices

We then tested the drug carbenoxolone, which is known to block gap junctions in a non-specific manner and has been observed to reduce seizure activity in animal models (Jin et al., 2011). Figure 6Aa showed a typical trace of spontaneous ictal/interictal-like discharges in a HH slice. Like mefloquine, carbenoxolone (10 or 100  $\mu\text{M}$ ) also dramatically eliminated these spontaneous ictal/interictal-like discharges (Fig. 6Ab,c), which was partially reversible after washout for 10–30 min (Fig. 6Ad). Again, like mefloquine, the carbenoxolone (100  $\mu\text{M}$ ) did not affect neuronal action potential firing in small HH neurons using patch-clamp recordings the HH slices from the same HH patient (Fig. 6B). We observed the suppression of ictal/interictal-like discharges in a concentration-dependent manner by examining the effect of carbenoxolone at three different concentrations. Compared with baseline level, the bursting numbers were reduced to  $81.5 \pm 7.1\%$ ,  $62.7 \pm 12.6\%$ , and  $11.5 \pm 7.4\%$  by 1  $\mu\text{M}$  ( $n = 3$  from 2 patients), 10  $\mu\text{M}$  ( $n = 3$  from 2 patients), and 100  $\mu\text{M}$  ( $n = 5$  from 4 patients) carbenoxolone, respectively. One-way ANOVA analysis indicated a highly significant difference of ictal/interictal-like discharges before and after carbenoxolone perfusion ( $F = 36.48$ ,  $p < 0.0001$ ). Post Tukey's analysis showed that 10 ( $p < 0.05$ ) and 100 ( $p < 0.001$ ), but not 1  $\mu\text{M}$  ( $p > 0.05$ ) of carbenoxolone significantly reduced seizure-burst frequency. These results further suggest that the block of gap junction (but not action potential firing of individual small HH neurons) by gap junction blocker (mefloquine or carbenoxolone) significantly reduced ictal/interictal-like discharges in human HH tissues.

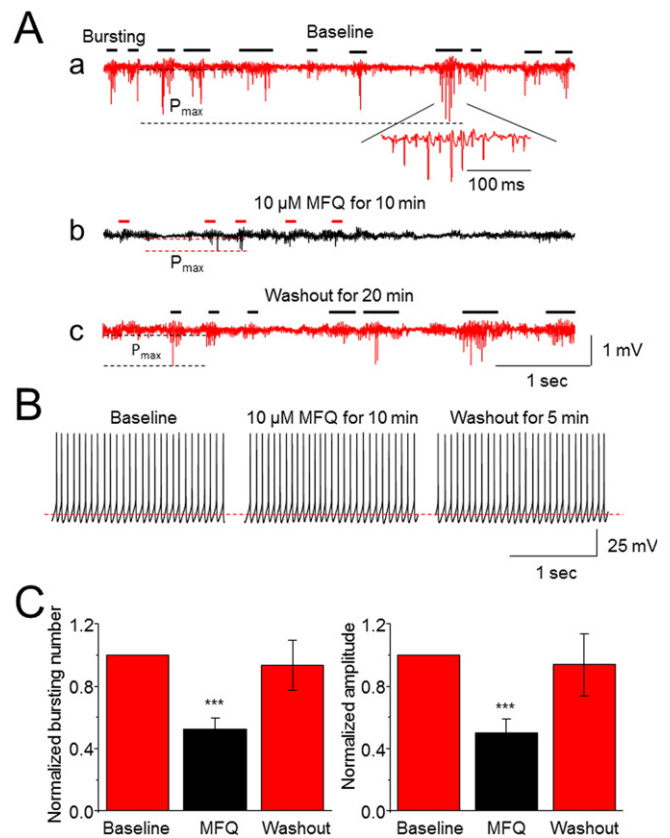


**Fig. 5.** Effects of neuronal-type gap-junction blocker on spontaneous ictal/interictal-like discharges in HH slices. (Aa) Representative typical trace of spontaneous ictal/interictal-like discharges of an HH slice (baseline). The bursting events are marked by horizontal bars, and the bursting maximum amplitudes ( $P_{\text{max}}$ ) are also indicated by two horizontal dashed lines. The lower trace (baseline, inset) shows an expanded bursting spike activity (from a selected discharge period) over a time demonstrating a  $\gamma$  range (60 Hz) spike-wave discharge. After bath perfusion of the neuronal-type gap-junction blocker, mefloquine (10  $\mu\text{M}$  for 10 min), the ictal/interictal-like discharges are reduced (Ab). After washout of mefloquine for 20 min, the seizure-like discharges are reversed (Ac). (B) Whole-cell patch-clamp recording represents a typical trace of spontaneous action potential firing of a small HH neuron from the HH slice collected from the same HH patient shown in Fig. 5A and demonstrate no change of exposure of 10  $\mu\text{M}$  mefloquine for 10 min. (C) Statistical analysis from eight HH slices (from four patients) shows that the neuronal-type gap-junction blocker significantly reduces both seizure bursting firing numbers and amplitude. \*\*\* $p < 0.001$ .

## 4. Discussion

Our results suggest that neuronal gap junctions between small HH neurons play a critical role in enabling synchrony of firing activity, thereby contributing to seizure-like discharges in HH. These results also suggest a potential strategy of using neuronal gap-junction blockers as therapeutic drugs to control seizure activity in HH patients with gelastic seizures.

How do these results contribute to the working model for epileptogenesis in HH tissue? Two predominant neuron phenotypes reside within HH tissue (Coons et al., 2007). The majority (approximately 90%) of HH neurons are small, round, monopolar or bipolar cells with local aspiny processes (Beggs et al., 2008; Coons et al., 2007; Kim do et al., 2008). These neurons express glutamic acid decarboxylase and project to symmetrical synapses; therefore, they are likely to be GABAergic interneurons (Beggs et al., 2008; Kim do et al., 2008; Wu et al., 2007; Wu et al., 2005). Small HH neurons occur in clusters that vary in size and abundance, but otherwise appear to be a universal feature of HH microarchitecture (Coons et al., 2007). Conversely, large HH neurons (approximately 10% of total) have a morphology consistent with projection-type cells, including a pyramidal shape, abundant Nissl substance, and multiple processes that are more highly branched and more

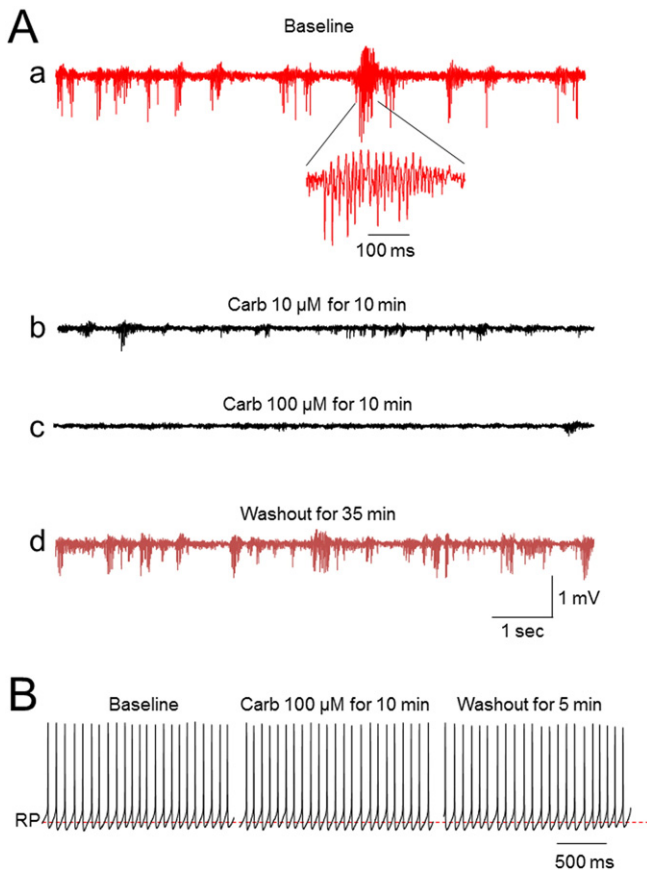


**Fig. 6.** (A) The microelectrode field recording of freshly resected, perfused HH tissue (slice thickness 450  $\mu\text{m}$ ) demonstrates spontaneous ictal/interictal-like discharges with the repetitive bursting (1–2 Hz) (baseline, Aa). The lower trace (baseline, inset) shows an expanded bursting spike activity (from a selected discharge period) over a time demonstrating a  $\gamma$  range (60 Hz) spike-wave discharge. Field recording from the same tissue slice after bath application of 10 or 100  $\mu\text{M}$  carbenoxolone (Carb) for 10 min both show a suppression of seizure-like discharges (A,b,c). The field recording from the same tissue slice after wash-out of carbenoxolone for 35 min shows partial recovery of the seizure-like discharges seen during the pre-application baseline (Ad). (B) Whole-cell patch-clamp recording in current-clamp mode from the same patient HH slice (different HH slices from field recording) demonstrates no detectable change of action potential firing of a small HH neuron observed before, during, and after 100  $\mu\text{M}$  carbenoxolone perfusion.

likely to be spiny (Beggs et al., 2008; Coons et al., 2007; Kim do et al., 2008).

Small HH neurons have spontaneous pacemaker-like firing resulting from intrinsic membrane properties (Kim do et al., 2008; Wu et al., 2007; Wu et al., 2008; Wu et al., 2005). Most large HH neurons exhibit a functionally immature response to GABA exposure, with depolarization and increased firing, resulting from reversal of the transmembrane chloride potential (Kim do et al., 2008; Kim et al., 2009; Wu et al., 2008). Taken together, these findings suggest a cellular model in which clusters of spontaneously firing interneurons paradoxically excite projection neurons in a functional network (Wu et al., 2015). There is indirect evidence for network activity within HH neuron clusters with microelectrode field recordings of high-frequency oscillations in perfused HH tissue slices (Simeone et al., 2011) and highly synchronous firing of single units with microelectrode field recordings in situ (prior to surgical resection) (Steinmetz et al., 2013).

Two basic cellular mechanisms are required for seizure activity—imbalance between excitatory and inhibitory influences with net excitation of the cellular network and enhanced synchrony of neuronal firing (Avoli et al., 2005). We hypothesized that synchrony of firing activity within HH tissue is mediated in part by non-synaptic mechanisms, specifically gap junctions, which are capable of electrically

linking adjacent neurons. In this study, we tested our hypothesis using multiple experimental approaches. The electron microscopy demonstrated an evidence of existence of gap junctions between small-sized GABA neurons in HH slices. The functional gap junctions between GABA neurons in HH slices were supported by microinjection of small HH neurons with biocytin via recording electrode under patch-clamp recording conditions demonstrates dye-coupling of adjacent neurons. Although the gap junctions are known to express in normal hypothalamic tissues (Condorelli et al., 2000), our Western-blot data showed a significant increase in expression level of Cx36 and Cx43 in HH tissue compared to normal control adjacent mammillary body tissue. These data suggest a possibility that enhanced gap junction proteins may promote GABA neuron synchronization and form the seizure-like discharges in HH lesion. This idea was further supported by electrophysiological experiments, in which, pharmacological blockade of gap junctions abolishes seizure-like discharges in freshly resected, perfused HH tissue slices without suppressing spontaneous single-unit firing activity. Our findings demonstrate the presence of neuronal gap junctions and suggest that gap junctions have a mechanistic role in generating seizure activity in HH tissue.

We acknowledge technical limitations to this study. We have utilized age-matched human autopsy hypothalamic tissue (mammillary body) as a control tissue for Western blots. We recommend mammillary body for control studies as this nucleus is immediately adjacent to all HH lesions associated with epilepsy (Parvizi et al., 2011) and it is readily identifiable in autopsy specimens. However, the embryological relationship between mammillary body and HH is unexplored and the cellular phenotypes are likely dissimilar. The increase of both Cx36 and Cx43 may relate to immature properties of HH tissue, as reflected by functional immaturity of large HH neurons with paradoxical excitation in response to GABA ligands. For our electrophysiological study with gap junction blockers, all comparisons were set up in the same recorded slice (or cell) before during and after gap junction blocker exposure. Another limitation is that we were not able to do in vivo study directly in HH patients in this paper. However, the intrinsic epileptic feature of HH allows us to test the role of gap junctions in epileptogenesis using HH slices, which provides significant insights into understanding of the impact of gap junctions in gelastic seizure genesis.

While providing new insights into the cellular mechanisms responsible for gelastic seizures arising in HH tissue, these results also suggest a novel approach to treatment, prompting research to evaluate the safety and efficacy of gap-junction blockers in HH patients. Gap-junction blockers are currently under investigation in people with migraines; the proposed mechanism in those studies is to attenuate or abolish cortical-spreading depression (Silberstein, 2009). Clear evidence for efficacy is thus far lacking, but gap-junction blockers appear to be safe and well tolerated. Based upon the findings reported here, we propose that gap-junction blockers are worthy of further investigation for treating seizures associated with HH and other types of epilepsy.

#### Author Contributions

Dr. Wu - study concept and design, acquisition of electrophysiology data, analysis and interpretation, statistical analysis, drafting and revising the manuscript.

Dr. Gao - acquisition of patch-clamp recording data, analysis and interpretation.

Stephen G. Rice - acquisition of immunohistochemical data, analysis and interpretation.

Candy Tsang - acquisition of Western-blot data, analysis and interpretation.

Dr. Beggs - acquisition of electron microscopy data, analysis and interpretation.

Dharshaun Turner - acquisition of slice field recording data, analysis and interpretation.

Guohui Li - acquisition of slice field recording data, analysis and interpretation.

Dr. Yang - study design, interpretation of the electrophysiology data, and revising the manuscript.

Dr. Xia - acquisition of slice field recording data and performed analysis.

Dr. Gao - Perform patch-clamp recordings from HH slices.

Dr. Qiu - study design, interpretation of the electrophysiology and cell biology data, and revising the manuscript.

Dr. Liu - acquisition of slice patch-clamp recording data, analysis and interpretation.

Dr. Kerrigan - study concept and design, acquisition of Western-blot data, data analysis and interpretation, statistical analysis, drafting and revising the manuscript.

## Disclosures

All authors report no disclosures.

## Acknowledgments

This work was supported by an NIH grant (NS-056,104, J.W.) and grants from the Barrow Neurological Foundation and Arizona Biomedical Research Commission (J.F.K., J.W.). Authors thank Dr. Xuesi Shao for his help to do statistical Chi square test. Study sponsors played no role in study design; collection, analysis, and interpretation of data; writing of the report; or the decision to submit this paper for publication

## References

- Avoli, M., Louvel, J., Pumain, R., Kohling, R., 2005. Cellular and molecular mechanisms of epilepsy in the human brain. *Prog. Neurobiol.* 77 (3), 166–200.
- Beggs, J., Nakada, S., Fenoglio, K., Wu, J., Coons, S., Kerrigan, J.F., 2008. Hypothalamic hamartomas associated with epilepsy: ultrastructural features. *J. Neuropathol. Exp. Neurol.* 67 (7), 657–668.
- Berkovic, S.F., Andermann, F., Melanson, D., Ethier, R.E., Feindel, W., Gloor, P., 1988. Hypothalamic hamartomas and ictal laughter: evolution of a characteristic epileptic syndrome and diagnostic value of magnetic resonance imaging. *Ann. Neurol.* 23 (5), 429–439.
- Carlen, P.L., Skinner, F., Zhang, L., Naus, C., Kushnir, M., Perez Velazquez, J.L., 2000. The role of gap junctions in seizures. *Brain Res. Brain Res. Rev.* 32 (1), 235–241.
- Condorelli, D.F., Belluardo, N., Trovato-Salinaro, A., Mudo, G., 2000. Expression of Cx36 in mammalian neurons. *Brain Res. Brain Res. Rev.* 32 (1), 72–85.
- Coons, S.W., ReKate, H.L., Prenger, E.C., Wang, N., Drees, C., Ng, Y.T., et al., 2007. The histopathology of hypothalamic hamartomas: study of 57 cases. *J. Neuropathol. Exp. Neurol.* 66 (2), 131–141.
- Cruikshank, S.J., Landisman, C.E., Mancilla, J.G., Connors, B.W., 2005. Connexon connexions in the thalamocortical system. *Prog. Brain Res.* 149, 41–57.
- Delalande, O., Fohlen, M., 2003. Disconnecting surgical treatment of hypothalamic hamartoma in children and adults with refractory epilepsy and proposal of a new classification. *Neurol. Med. Chir.* 43 (2), 61–68.
- Dudek, F.E., Yasumura, T., Rash, J.E., 1998. 'Non-synaptic' mechanisms in seizures and epileptogenesis. *Cell Biol. Int.* 22 (11–12), 793–805.
- Jin, M.M., Chen, Z., 2011. Role of gap junctions in epilepsy. *Neurosci. Bull.* 27 (6), 389–406.
- Juszczak, G.R., Swiergiel, A.H., 2009. Properties of gap junction blockers and their behavioural, cognitive and electrophysiological effects: animal and human studies. *Prog. Neuro-Psychopharmacol. Biol. Psychiatry* 33 (2), 181–198.
- Kerrigan, J.F., Ng, Y.T., Chung, S., ReKate, H.L., 2005. The hypothalamic hamartoma: a model of subcortical epileptogenesis and encephalopathy. *Semin. Pediatr. Neurol.* 12 (2), 119–131.
- Kim, D.Y., Fenoglio, K.A., Kerrigan, J.F., Rho, J.M., 2009. Bicarbonate contributes to GABA<sub>A</sub> receptor-mediated neuronal excitation in surgically resected human hypothalamic hamartomas. *Epilepsy Res.* 83 (1), 89–93.
- Kim, D.Y., Fenoglio, K.A., Simeone, T.A., Coons, S.W., Wu, J., Chang, Y., et al., 2008. GABA<sub>A</sub> receptor-mediated activation of L-type calcium channels induces neuronal excitation in surgically resected human hypothalamic hamartomas. *Epilepsia* 49 (5), 861–871.
- Kuzniecky, R., Guthrie, B., Mountz, J., Bebin, M., Faught, E., Gilliam, F., et al., 1997. Intrinsic epileptogenesis of hypothalamic hamartomas in gelastic epilepsy. *Ann. Neurol.* 42 (1), 60–67.
- Mittal, S., Mittal, M., Montes, J.L., Farmer, J.P., Andermann, F., 2013. Hypothalamic hamartomas. Part 2. Surgical considerations and outcome. *Neurosurg. Focus.* 34 (6), E7.
- Munari, C., Kahane, P., Francione, S., Hoffmann, D., Tassi, L., Cusmai, R., et al., 1995. Role of the hypothalamic hamartoma in the genesis of gelastic fits (a video-stereo-EEG study). *Electroencephalogr. Clin. Neurophysiol.* 95 (3), 154–160.
- Nakase, T., Naus, C.C., 2004. Gap junctions and neurological disorders of the central nervous system. *Biochim. Biophys. Acta* 1662 (1–2), 149–158.
- Parvizi, J., Le, S., Foster, B.L., Bourgeois, B., Rivello, J.J., Prenger, E., et al., 2011. Gelastic epilepsy and hypothalamic hamartomas: neuroanatomical analysis of brain lesions in 100 patients. *Brain J. Neurol.* 134 (Pt 10), 2960–2968.
- Prigatano, G.P., Wethe, J.V., Gray, J.A., Wang, N., Chung, S., Ng, Y.T., et al., 2008. Intellectual functioning in presurgical patients with hypothalamic hamartoma and refractory epilepsy. *Epilepsy Behav.* 13 (1), 149–155.
- Roopun, A.K., Simonotto, J.D., Pierce, M.L., Jenkins, A., Nicholson, C., Schofield, I.S., et al., 2010. A nonsynaptic mechanism underlying interictal discharges in human epileptic neocortex. *Proc. Natl. Acad. Sci. U. S. A.* 107 (1), 338–343.
- Rozental, R., Giaume, C., Spray, D.C., 2000. Gap junctions in the nervous system. *Brain Res. Brain Res. Rev.* 32 (1), 11–15.
- Silberstein, S.D., 2009. Tonabersat, a novel gap-junction modulator for the prevention of migraine. *Cephalalgia Int. J. Headache* 29 (Suppl. 2), 28–35.
- Simeone, K.A., Sabesan, S., Kim, D.Y., Kerrigan, J.F., Rho, J.M., Simeone, T.A., 2011. L-Type calcium channel blockade reduces network activity in human epileptic hypothalamic hamartoma tissue. *Epilepsia* 52 (3), 531–540.
- Sohl, G., Maxeiner, S., Willecke, K., 2005. Expression and functions of neuronal gap junctions. *Nat. Rev. Neurosci.* 6 (3), 191–200.
- Steinmetz, P.N., Wait, S.D., Lekovic, G.P., ReKate, H.L., Kerrigan, J.F., 2013. Firing behavior and network activity of single neurons in human epileptic hypothalamic hamartoma. *Front. Neurol.* 4, 210.
- Traub, R.D., Michelson-Law, H., Bibbig, A.E., Buhl, E.H., Whittington, M.A., 2004. Gap junctions, fast oscillations and the initiation of seizures. *Adv. Exp. Med. Biol.* 548, 110–122.
- Wu, J., Chang, Y., Li, G., Xue, F., DeChon, J., Ellsworth, K., et al., 2007. Electrophysiological properties and subunit composition of GABA<sub>A</sub> receptors in patients with gelastic seizures and hypothalamic hamartoma. *J. Neurophysiol.* 98 (1), 5–15.
- Wu, J., DeChon, J., Xue, F., Li, G., Ellsworth, K., Gao, M., et al., 2008. GABA(A) receptor-mediated excitation in dissociated neurons from human hypothalamic hamartomas. *Exp. Neurol.* 213 (2), 397–404.
- Wu, J., Gao, M., Shen, J.X., Qiu, S.F., Kerrigan, J.F., 2015. Mechanisms of intrinsic epileptogenesis in human gelastic seizures with hypothalamic hamartoma. *CNS Neurosci. Ther.* 21 (2), 104–111.
- Wu, J., Xu, L., Kim, D.Y., Rho, J.M., St John, P.A., Lue, L.F., et al., 2005. Electrophysiological properties of human hypothalamic hamartomas. *Ann. Neurol.* 58 (3), 371–382.